Contents lists available at ScienceDirect

EBioMedicine

Research paper

Identification of novel biomarkers for arthrofibrosis after total knee arthroplasty in animal models and clinical patients

Xi Chen[a,b], Zhaolun Wang[a], Yong Huang[a], Wang Deng[a], Yixin Zhou[a,*], Ming Chu[b,*]

[a] Department of Adult Joint Reconstructive Surgery, Beijing Jishuitan Hospital, Fourth Clinical College of Peking University, Jishuitan Orthopaedic College of Tsinghua University, 31 East Xinjiekou Street, Beijing 100035, China
[b] Department of Immunology, School of Basic Medical Sciences, Peking University. NHC Key Laboratory of Medical Immunology (Peking University). Beijing, China

ARTICLE INFO

ABSTRACT

Background: Arthrofibrosis is a debilitating complication after total knee arthroplasty (TKA) which becomes a considerable burden for both patients and clinical practitioners. Our study aimed to identify novel biomarkers and therapeutic targets for drug discovery.

Methods: Potential biomarker genes were identified based on bioinformatic analysis. Twelve male New Zealand white rabbits underwent surgical fixation of unilateral knees to mimics the joint immobilization of the clinical scenario after TKA surgery. Macroscopic assessment, hydroxyproline content determination, and histological analysis of tissue were performed separately after 3-days, 1-week, 2-weeks, and 4-weeks of fixation. We also enrolled 46 arthrofibrosis patients and 92 controls to test the biomarkers. Clinical information such as sex, age, range of motion (ROM), and visual analogue scale (VAS) was collected by experienced surgeons

Findings: Base on bioinformatic analysis, transforming growth factor-beta receptor 1 (TGFBR1) was identified as the potential biomarkers. The level of TGFBR1 was significantly raised in the rabbit synovial tissue after 4-weeks of fixation ($p<0.05$). TGFBR1 also displayed a highly positive correlation with ROM loss and hydroxyproline contents in the animal model. TGFBR1 showed a significantly higher expression level in arthrofibrosis patients with a receiver operating characteristic (ROC) area under curve (AUC) of 0.838. TGFBR1 also performed positive correlations with VAS baseline (0.83) and VAS after 1 year (0.76) while negatively correlated with ROM baseline (-0.76) in clinical patients.

Interpretation: Our findings provided novel biomarkers for arthrofibrosis diagnosis and uncovered the role of TGFBR1. This may contribute to arthrofibrosis prevention and therapeutic drug discovery.

1. Introduction

Arthrofibrosis (AF) is a well-known devastating postoperative complication after the total knee arthroplasty (TKA) which can be characterized by the excessive production of collagen resulting in fibrous scar tissue in the joint [1]. The proliferated fibrous scar tissue forms adhesions in knee joint capsules, tendons, and bursa around the joint, which leads to restricted joint motion and knee pain [2].

The prevalence of arthrofibrosis after TKA ranges from 1 to 17% [3−6], which causes significant disability and limitation in daily living. Even a small loss of 5° of knee flexion will seriously affect physical activities of patients and create considerable difficulties in sitting, driving, and stair climbing [7]. Together with the loss of ROM, constant pain of the knees was also commonly reported by the patients, which lead to a large proportion of revision surgery and places a heavy economic burden on the health care system [4].

Unfortunately, the conservative treatments to prevent the AF in the early stage are largely unknown due to the lack of specific biomarkers and reliable therapeutic targets. As the primary concerns in joint surgery, a plethora of attempts have been made to discover biomarkers. The first biomarker of arthrofibrosis, α-SMA (ASMA), was identified early in 2003 in the myofibroblasts [8] and performed significant difference in the AF patients compared to controls [9,10]. Beta-catenin was also defined as a reference for AF diagnosis and severity grading in 2013 by Ruppert and colleagues [9]. Besides, CD68 expressed in the sublining layer of synovial was known as the biomarker for diagnosis and indicator of inflammatory activity [10,11]. Matrix metalloproteinases (MMPs), tissue inhibitors of matrix metalloproteinases (TIMPs), and a disintegrin and metalloproteinases with thrombospondin (ADAMTS) also show clinical relevance of knee stiffness after TKA [12].

* Corresponding author.
E-mail addresses: orthoyixin@yahoo.com (Y. Zhou), famous@bjmu.edu.cn (M. Chu).

Despite the increase of AF biomarkers, there is still lack of highly specific and sensitive biomarkers for clinical use. Comprehensive molecular analyses of AF are needed for novel biomarker identification and therapeutic targets investigation. Recently, Banu Bayram and colleagues had successfully performed RNA-sequencing of posterior capsule specimens from 4 patients undergoing a revision total knee arthroplasty (TKA) for arthrofibrosis (RTKA-A) and 4 patients for non-arthrofibrotic and non-infectious etiologies (RTKA-NA) [13]. This finding uncovered the molecular changes in arthrofibrosis tissue and shed light on the biomarkers for diagnosis in the clinical scenario.

The purpose of this study was to identify the biomarker genes from this expression data (GSE135854), validated in animal models, and applied in clinical patients with both clinical symptoms and pathological confirmation of arthrofibrosis. Herein, we established a classic rabbit model of AF which had been widely used in other studies [14–19]. Comparing with other animal models, rabbits are more reliable for joint fibrosis formation after fixation and more effective in measurement [14,20]. They also shared a similar knee anatomy structure as humans which were convenient for surgical procedure and synovial tissue obtain. In this study, we immobilized the knees for different time span (3-days, 1-week, 2-weeks, and 4-weeks) to explore the biomarker gene expression over time.

This study aimed to bridge between the bioinformatics analyses and clinical scenarios. In clinical practice, these biomarkers information can be easily obtained during the treatment of arthrofibrosis such as revision TKA, arthroscopic, open lysis of adhesions, and manipulation under anesthesia (MUA). Our study may pave a new way for precise diagnosis and drug discovery of patients with AF after TKA.

2. Methods

2.1. Statement of ethics

This study was designed and performed according to the registration and had been approved by the Ethic Committee of Jishuitan hospital (No.201811−09). All animal experiments were carried out with the Guide for the Care and Use of Laboratory Animals of the National Institutes of Health [21]. The case-control study part was also conducted with the permission of the Ethics Committee of the Jishuitan hospital (No.202011−02) and informed consent was received from the patients. For those who cannot write properly, the informed consent form was signed by their lineal relatives.

2.2. Gene expression omnibus data set selection

The gene profiles were downloaded for The gene expression omnibus database (GEO, http://www.ncbi.nlm.nih.gov/geo) to explore the early-stage diagnostic biomarker after TKA. Finally, we selected GSE135854 based on the platforms of GPL18573 Illumina NextSeq 500 (Homo sapiens) for further investigation [13]. GSE135854 contained 4 patients with arthrofibrosis in their knee joint after TKA and 4 patients without arthrofibrosis after TKA as control. All these samples were standardized by the affy package of R programming software. (https://www.r-project.org/)

2.3. Differentially expressed genes (DEGs) Identification

Differentially expressed genes (DEGs) were identified with Bioconductor's package Limma package of R programming software in this study. The criteria for DEGs in these two profiles was set as the adjusted P-value < 0.05 (Benjamini-Hochberg method) or |logFC| > 1 based on the Bayes' test. Hierarchical clustering analysis were identified by the pheatmap packages R programming software [22]. The shared DEGs were also shown with a Venn diagram (http://bioinfogp.cnb.csic.es/tools/venny/).

2.4. GO and KEGG analysis

Gene ontology and pathway enrichment analysis of these two gene profiles DEGs were conducted with the clusterProfiler packages of R programming software. As the enrichment functions of DEGs analysis, Go terms and KEGG pathway with FDR<0.05 were selected.

2.5. PPI network integration

Protein-protein interaction (PPI) of the DEGs of these two profiles and the shared DEGs were constructed by Search Tool for the Retrieval of Interacting Genes database (STRING, https://string-db.org/) [23]. Interactions possibility in STRING is quantified with four levels of confidence score (highest>0.9, high>0.7, medium>0.4, low>0.15) [24]. We set the high confidence score (>0.7) to have the best visual performance of the network integration.

2.6. The surgical procedure of animal model

All animal models were established in accordance with the institutional animal research ethic and international guidelines. Twelve male New Zealand white rabbits (mean weight 2.5 kg) were randomly and equally divided into 4 groups by immobilization time: 3-days groups, 1-week groups, 2 weeks groups, and 4 weeks groups to explore the time sequence of gene expression. After anesthetized by intravenous injection of 20% urethane, the animals' surgery was performed according to the previous protocol [25]. Briefly, the fur around the right knee was shaved and the exposed skin was sterilized using iodophor. The surgical limbs in each group were immobilized by 1.2 mm Kirschner wires (K-wire) in the fully flexed position for 3-days, 1 week, 2 weeks groups, and 4 weeks groups. The animals after surgery were kept individually in cages that had full access to standard chow and water.

2.7. Measurement of the ROM

The rabbits were humanely euthanized by intravenous administration of 20% urethane (5 g/kg) at the endpoint of each group. [16,19]After the K-wires were removed, the range of motion of the fixed knees and the control knees were measured according to the previous studies. With a looped wire hooked on the distal leg, which was 8 cm distal from the proximal tibia joint surface. A consistent force of 5 N was applied to the looped wire and the angle of femur and tibia was measured as the ROM.

2.8. Determination of hydroxyproline content

The synovial membrane and fibrous scars were removed from both knees and 20 mg (wet weight) of the tissue were used as hydroxyproline content determination samples. As the previous study described [16], the samples were hydrolyzed with 6 mol/l HCl at 130°C for 12 h and then neutralized with 2.5-N NaOH, which methyl red was apply as the indicator. With 1 ml of chloramine T added, all the tissue samples and four known hydroxyproline standards were incubated for 20 min at room temperature. Subsequently, 1 ml p-dimethylaminobenzaldehyde solution was added in both sample and standards. With the spectrophotometer, the absorbance of the solution was determined at 558 nm. Based on the standard curve, the hydroxyproline content of the sample was calculated.

2.9. Histological analysis

The synovial membrane and fibrous scars removed from 24 knees were fixed in the 10% buffered formalin and then embedded in paraffin. A total of 24 4-μm transverse sections which were perpendicular to the femoral axis were obtained and stained with hematoxylin-eosin. The synovial membrane and fibrous scar tissue were evaluated under microscopy at $\times$ 100 magnification. The histological images at $\times$ 400 magnification were obtained by the digital scanner (KF-PRO-005 Magscanner).

2.10. Immunohistochemistry evaluation

Immunohistochemical stains were performed with an automated immunostainer (Autostainer 720, Labvision) according to standard heat-induced epitope retrieval and the avidin-biotin-peroxidase complex method. Antibodies used in the present study are α-SMA (Abcam CAT#ab32575, RRID: AB_722,538), TGFBR1 (Abcam CAT#ab31013, RRID: AB_778,352), TGFBR2 (Abcam CAT#ab186838, RRID: AB_2,728,775), which have been validated the pilot study beforehand. Sections were incubated overnight at 4°C and were counterstained with Hematoxylin (Thermo Electron Corporation, Pittsburgh, PA, US). The scoring procedure was applied as the

previous studies mentioned about [26]. Two pathologists evaluated independently without informed of the group information beforehand. About 100 fibroblasts stained positively filed were defined as target filed which the percentage of total cells were carefully inspected. The Kruskal-Wallis test was applied to determine the difference between these groups. In this study, we set p-value<0.05 as statistically significant.

2.11. RT-PCR

TRIzol® Reagent (Plant RNA Purification Reagentfor plant tissue) was used to isolate the RNA in these capsules and synovial membrane of each knee. The quality of the extracted RNA was determined by 2100 Bioanalyser (Agilent) and quantified with the ND-2000 (Nano-Drop Technologies). RevertAid First Strand cDNA Synthesis Kit (Thermo Scientific, San Jose, CA) was applied to get the reverse transcription in accordance with the standard instructions. Specific primers (GAPDH: F—TCA CCA TCT TCC AGG AGC GA and R—CAC AAT GCC GAA GTG GTC GT; ACTA2(a-SMA) F—GACCGAATGCAGAAGGAG R—CGGTGGACAATGGAAGG; TGFBR1 (ALK5) F—CGACGGCGTTA-CAGTGTTTCT R—CCCATCTGTCACACAAGTAAA; ACVRL1 (ALK1) F—CCATCGTGAATGGCATCGT R—GGTCATTGGGCACCACATC) were selected as the previous studies mentioned [27].

2.12. Patients' enrollment and Intraoperatively samples collection

The present case-control study was conducted in accordance with the Strengthening the Reporting of Observational Studies in Epidemiology (STROBE) [28]. All the patients' information in the pathology medical records database (PMRD) was screened. A total of 758 patients who underwent revision knee surgery in the Department of Adult Joint Reconstructive Surgery of Jishuitan hospital from January 2010 to April 2020 were evaluated. Among them, 46 patients were further enrolled according to the inclusion criteria and exclusion criteria (Table 1) [5,29,30]. The arthrofibrosis of this study was defined as the limited range of motion (flexion ROM<90 degree) due to the soft-tissue fibrosis. In addition, another 92 patients in the PMRD were also enrolled as a control group by individual matching according to sex and age groups (40−49, 50−59, 60−69, 70−79, and ≥80 years) (1:2 ratio). As one of the major complaints of the AF patients, knee pain was also taken into consideration in this study. A visual analogue scale (VAS) was applied in this study for the knee pain measurement [31]. The score of VAS ranges from 0 to 10, with higher scores indicating worse knee pain. Baseline clinical information such as sex, age, range of motion (ROM), and visual analogue scale (VAS) was collected and evaluated by experienced surgeons before the surgery. The ROM and VAS after surgery were collected with at least 1-year follow-up by the same surgeons. Synovial tissue was collected during the revision operation process with patients' informed consent. After fixed in 10% buffered formalin and embedded in the paraffin, this synovial tissue was kept in the sample bank of the JST hospital pathology department. Subsequently, immunohistochemis-

Table 1
Inclusive and exclusive criteria of the AF patients.

Number	Inclusive criteria	Exclusive criteria
1	Persistent limitation of flexion ROM<90° at minimum 1 year follow-up	Prosthetic joint infection
2	Revision of TKA surgery for high degree of psychological strain and restriction of quality of life	Revision of TKA surgery for instability or loosening of the implantation
3	Inform consent of the patients	No obvious fibrous tissue under the microscope

try and Histological evaluation of the obtained samples was performed as previously mentioned.

2.13. Statistical analysis

Clinical measurement data were reported with a mean, standard deviation, and 95% confidence interval (CI). All analyses in this study were calculated in *R* programming software (version 3.6.2) and used the tidyverse workflow [32]. The chi-squared test and *t*-test were applied for the comparison between two groups of categorical variables and continuous variables separately. Correlation analyses were conducted with the Corrplot package of *R* programming software

[33] (https://github.com/taiyun/corrplot). ROC curves were depicted and the area under the curve (AUC) was calculated based on the pROC package of R programming software [34]. The cut-off value in this study was defined as the value which corresponded to the maximum joint sensitivity and specificity on the ROC curve. The significant level was set to a *P*-value of <0.05 in all statistical analyses.

2.14. Role of funding source

Funders of this study had no role in study design, data collection, data analyses, interpretation, or writing of the report.
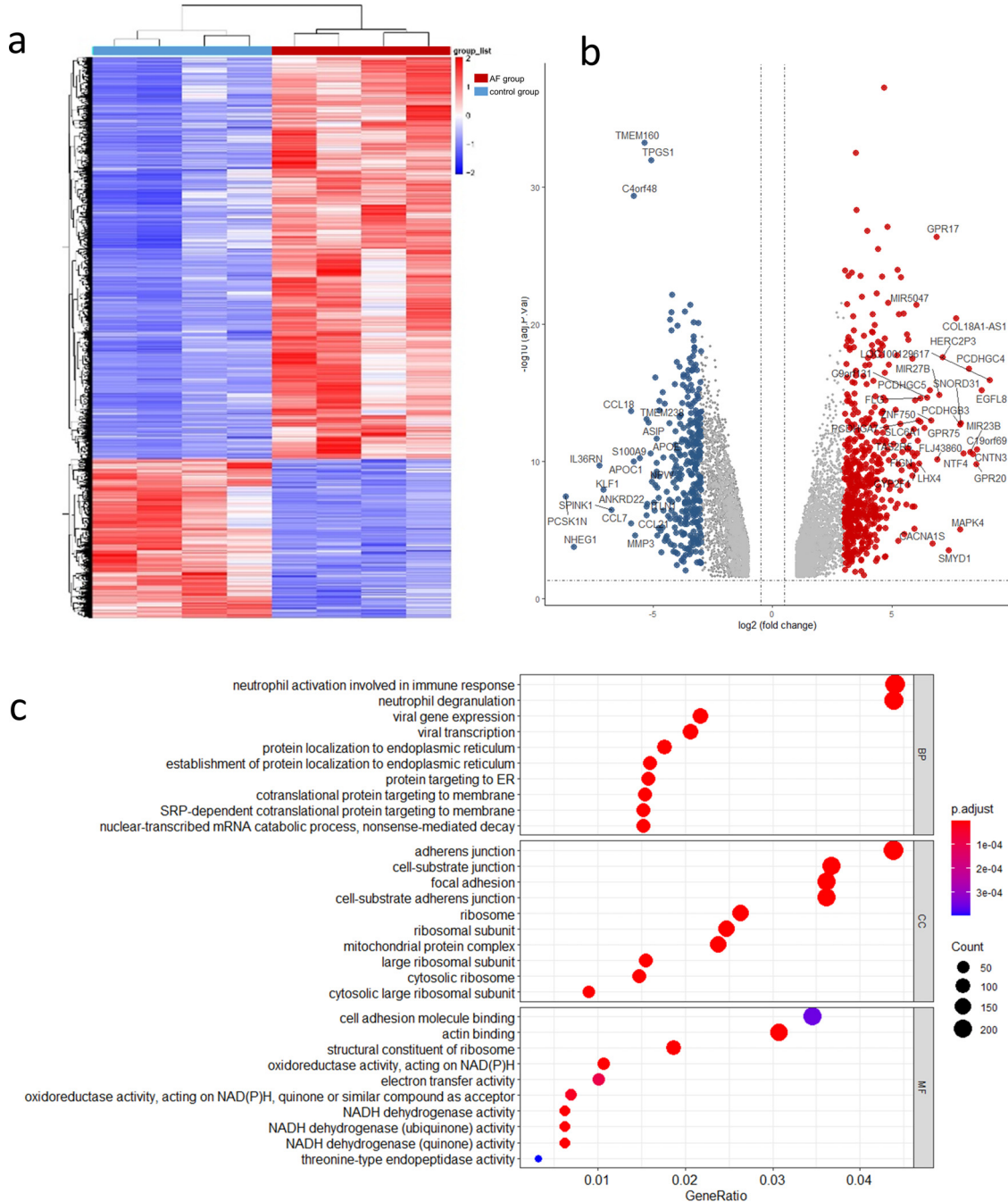
Fig. 1. Identification of differentially expressed genes (DEGs).

(a) Hierarchical clustering analysis of the DEGs between 4 RTKA-A and 4 RTKA-NA patients.

(b) Volcano plot of the DEGs. The red points and blue points represented the significantly up and down-regulated genes (|LogFC|>2).

(c)Gene ontology analysis of the DEGs. The size of the spot represents the gene counts and the color represents the adjusted p-value (Benjamini-Hochberg method) (For interpretation of the references to color in this figure legend, the reader is referred to the web version of this article.).

Table 2
Fibrotic genes involve in the arthrofibrosis.

Number	Key genes	Published year	Author
1	AEN, CARD11, DAD1, DDR2, EIF3E, EPDR1, FBXL7, FBXO45, ITGA11, KRT15, KRT19, MAFB, MMP14, MMP21/22B, SAV1, TIMP2, TMEM170A	2020	Wanget al. [15]
2	Eotaxin3, IL-5, IL12_23p40, IP10, VEGF, IL-7, IL-12p70, IL-16 and IL-17a	2020	Mann et al. [12]
3	CD68, ASMA, beta-catenin and BMP-2	2019	Sun et al. [16]
4	MMPs, TIMPs and ADAMTS	2019	Unterhauser et al. [8]
5	GRP78, CHOP and Bcl-2	2019	Arsoy et al. [17]
6	Type I collagen, α-SMA and GRP78, ATF6α, XBP1s	2018	Zhou and Yang [18]
7	types I and III collagen,HIF-1α,TGF-b and TGF-SS1	2017	Zhou at al. [19]
8	MCP-1, leptin, VEGF, IL-1β, IL-16 and IL-18	2016	Hazlewood et al. [20]
9	CTGF,VEGF and HIF-1	2016	National Research Council [21]
10	GMCSF, IL-1R1, IL-6 and IL-8	2015	Kolde [22]

3. Results

3.1. Identification of differentially expressed genes (DEGs)

We inspected the RNA-sequencing data (GSE135854) of posterior capsule specimens from 4 RTKA-A and 4 RTKA-NA patients and identified 6104 differentially expressed genes (3165 up-regulated and 2939 down-regulated DEGs). These results were displayed by heatmap in Fig. 1a and volcano plot in Fig. 1b. All of these up and down-regulated fibrosis DEGs were displayed in Supplementary Table 1.

Gene ontology analyses were subsequently performed to explore the function of these DEGs (Fig. 1c). The immune response of the neutrophil activation ranked highest in the biological process (BP) enrichment analysis which may correlate with the knee infection after the total knee arthroplasty. Consistently with our expectancy, adherens junction and cell adhesion molecule binding took precedence in both cellular components (CC) and molecular function (MF). These results demonstrated that these DEGs were preliminary candidates of the fibrosis biomarker gene for further study.

3.2. Discovery of potential arthrofibrosis biomarker genes (PABGs)

To explore the reliable biomarkers of arthrofibrosis after the total knee arthroplasty, a total of 151 fibrotic genes list (FBGs) was constructed based on the literature searching. Results from joint contractures or knee stiffness studies were enrolled and these fibrotic genes were listed in Table 2, including COL3A1, COL1A1, ACTA2, CD68, BMP2, TGF-β, etc. A total of 63 potential arthrofibrosis biomarker genes (PABGs) was obtained after DEGs overlapped with the fibrosis biomarker genes database (FBGs) (Fig. 2a). PABGs genes, including 50 up-regulated and 13 down-regulated genes, were listed in Supplementary Table 2. Gene ontology analysis in Fig. 2B also confirmed that the PABGs were the promising candidate of the fibrosis biomarker genes. The correlation matrix was depicted in Fig. 2d to have an overview of these PABGs. STRING protein-protein interaction (PPI) of the potential arthrofibrosis biomarker genes (PABGs) was showed in Fig. 2C. This PPI network consisted of 3 major subgroups (MMPs, COLs, and ADAMTS) and several central hub genes including TGFBR1 and TGFBR2.

As the central hub genes, TGFBR1 and TGFBR2 performed positive correlations with fibrotic genes (COLs and ADAMTS) while negatively correlated with anti-fibrotic genes (MMP24) (Fig. 2e). The expression of these genes was showed in Fig. 2F and subsequently selected for further validation in animal models.

3.3. Validation of arthrofibrosis biomarkers in animal model

12 rabbits in this study were divided into four groups and immobilized for 3-days, 1 week, 2 weeks, and 4 weeks with K-wires. The knee flexion ROM of these four groups was illustrated in Fig. 3c (3 days, control group 143$\pm$4°; fixation group 141$\pm$3°;1-week, control

group 139$\pm$4°; fixation group 121$\pm$5°;2 weeks, control group 137$\pm$6°; fixation group 86$\pm$8°;4 weeks, control group 132$\pm$7°; fixation group 52$\pm$6°). The knee flexion ROM in the fixation groups was remarkably decreased after 2 weeks of immobilization comparing with the control groups based on Mann-Whitney U test (p<0.05). Consistently with the ROM data, the hydroxyproline contents also showed a sharp contrast after 2 weeks of immobilization between the fixation groups and the control groups. The representative histological slices also delineated the dynamic process of arthrofibrosis in the rabbits' knee joint from another perspective (Fig. 3e).

To explore the correlation between arthrofibrosis and the selected biomarkers, the average mRNA levels of TGFBR1 and TGFBR2 were measured by RT-PCR (Fig. 4a and d). The mRNA of TGFBR1 up-regulated from over 2-fold at week 1 to 5-fold at week 4. The mRNA of TGFBR2 increased sharply from the two weeks after immobilization. In addition, these mRNA expressions of TGFBR1 and TGFBR2 both perform a strong negative correlation between ROM and a positive correlation between hydroxyproline contents (Fig. 4b−f). These results in the animal proved that TGFBR1 and TGFBR2 are dependable indicators to manifest the knee joint ROM which may be great biomarkers for clinical use.

3.4. Validation of arthrofibrosis biomarkers in patients

In order to validate these biomarker genes in clinical scenario, a total of 46 patients who underwent revision TKA surgery with both clinical symptoms and pathological confirmation of arthrofibrosis were enrolled as the arthrofibrosis group. While 92 patients with non-arthrofibrotic and non-infectious etiologies after revision TKA surgery were also invited as the control groups matched by sex and age groups. The baseline information of these two groups including the age, sex, BMI, baseline VAS and baseline flexion ROM before the revision surgery were showed in Table 3. There was no significant difference between these two groups except the baseline flexion ROM and VAS before revision surgery. The synovial membrane tissue and the fibrous scar tissue were obtained intraoperatively with the informed consent of the patients. Representative histological slides were shown in Fig. 5a, which were stained by Hematoxylin-Eosin and immunohistochemistry. Based on these slices, the Immunohistochemical scores of TGFBR1 and TGFBR2 graded from 0 to 5 were evaluated by two independent pathologists. The α-SMA was also involved as a reference indicator since the α-SMA was the specific marker of myofibroblast cells reported in the previous studies [9]. The Violin plots of the TGFBR1, TGFBR2 and α-SMA Immunohistochemical score (Fig. 5b−d) showed significant differences between the arthrofibrosis group and the control group (Mann-Whitney U-test p-value<0.05). In order to have a clear exploration of these biomarkers for arthrofibrosis diagnosis, the ROC curves were depicted in Fig. 6a. The area under curve (AUC) of TGFBR1, TGFBR2, and α-SMA score model were 0.838, 0.777, and 0.711 separately (Table 4). The value of 1.5 in the Immunohistochemical score of TGFBR1
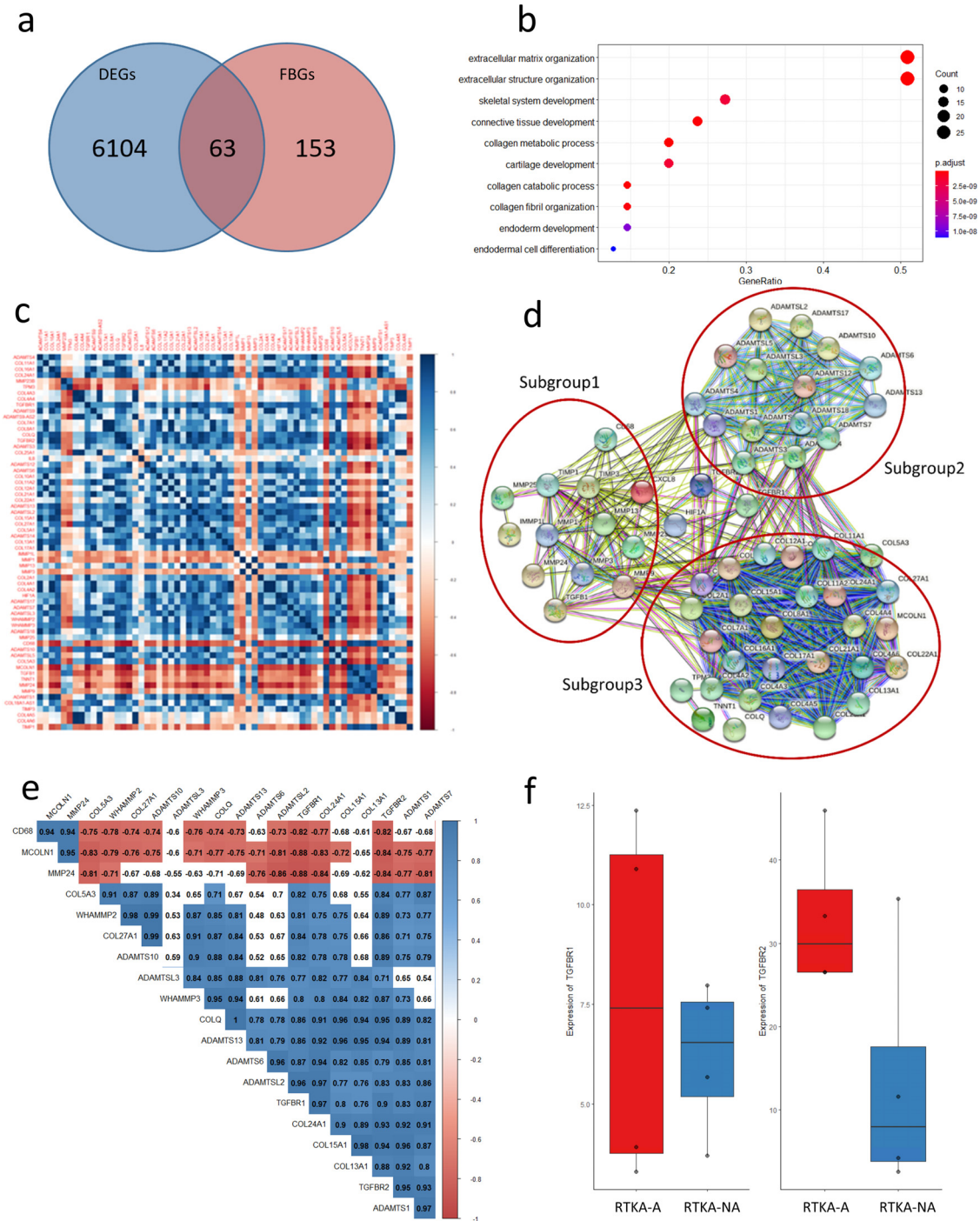
Fig. 2. Analysis of the potential arthrofibrosis biomarker genes (PABGs).

(a) Venn diagram of DEGs overlapped with fibrosis biomarker genes database (FBGs)

(b) Gene ontology analysis of the potential arthrofibrosis biomarker genes (PABGs). The size of the spot represents the gene counts and the color represents the adjusted *p*-value (Benjamini-Hochberg method).

(c) Correlation coefficient matrix of PABGs.

(d) STRING protein−protein interaction (PPI) network of PABGs

(e) High correlated genes matrix of PABGs.

(f) Expression of TGFBR1 and TGFBR2 in arthrofibrosis group and control group.

corresponded to the maximum joint sensitivity and specificity on the ROC curve (63.8% sensitivity and 91.3% specificity), which was defined as the cut-off value. As such, the TGFBR1 score model performed the best among these diagnostic models in the ROC analysis.

To have a deep insight into these three biomarkers, the clinical outcome follow-up information of the arthrofibrosis group patients were applied, including ROM before revision surgery, VAS before

revision surgery, ROM 1 year after the revision surgery, and VAS 1 year after the revision surgeries. Correlation coefficients were calculated between these biomarkers and clinical outcomes. (Fig. 6b) TGFBR1 had positive correlation coefficients with VAS baseline (0.83) and VAS after 1 year of revision TKA (0.75), and it was also negatively correlated with ROM baseline (-0.76). These results were also delineated in Fig. 6c to have a particular view in the scatter plots. With
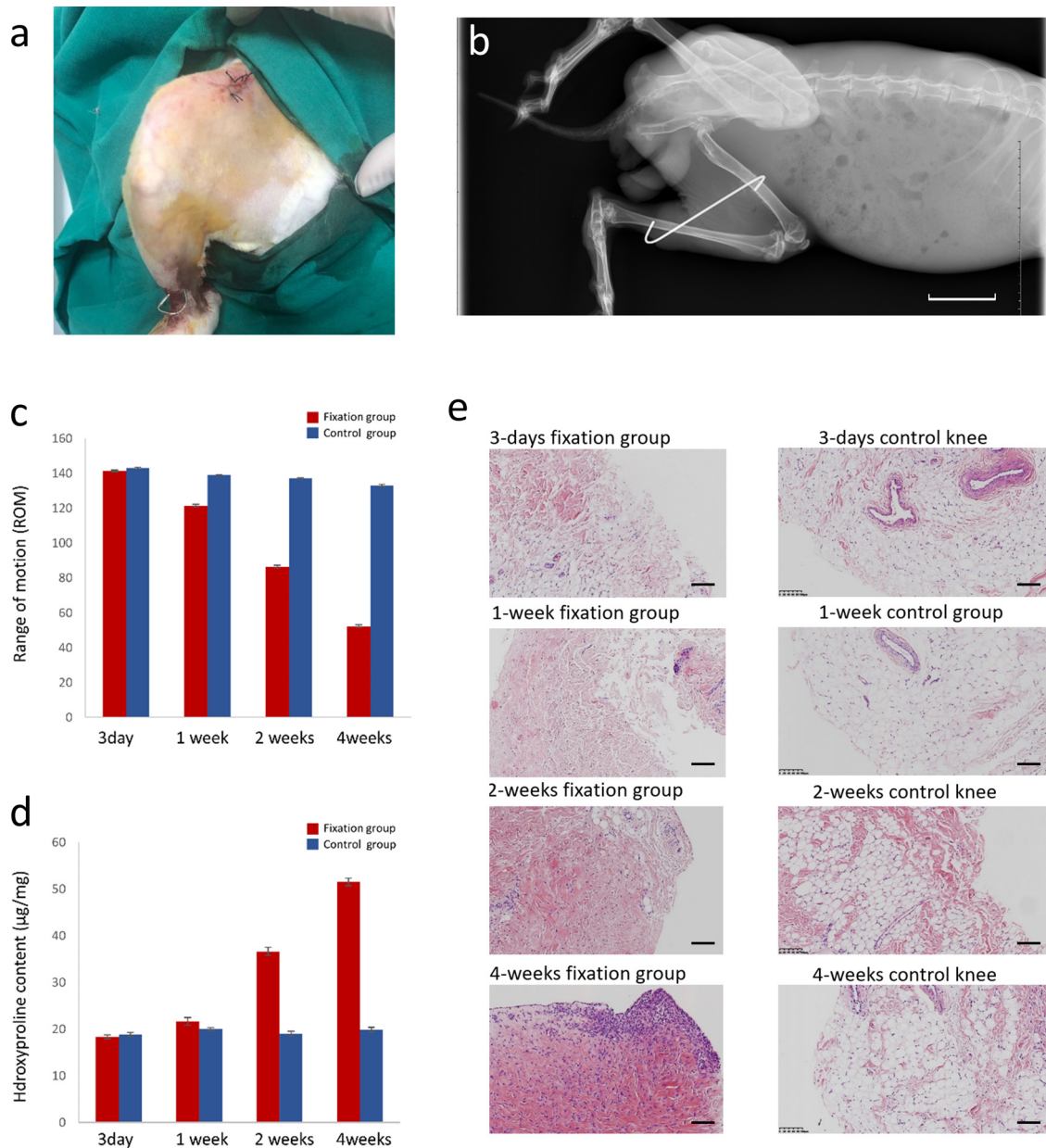
Fig. 3. Establishment of arthrofibrosis animal model.

(a) Representative photo of rabbit knee after the fixation surgery.

(b) Representative X-ray photo of rabbit fixation knee (lower leg) and control knee (upper leg). Bar= 5cm

(c,d) Comparison of the range of motion (ROM) and hydroxyproline contents in the fixation and control groups (*n*=12). 3 days= rabbit underwent 3 days immobilization; 1 week = rabbit underwent 1 week immobilization; 2 weeks = rabbit underwent 2 weeks immobilization; 4 weeks = rabbit underwent 4 weeks immobilization; Each time point group have 3 biological replicates. Error bars indicate the standard deviations.

(e) Representative histological slices of rabbits' knees in the control and fixation groups for 3-days, 1-week, 2-weeks, and 4weeks. Bar= 200 μm.

this, we proposed that TGFBR1 was a relatively accurate indicator for AF diagnosis and severity grading.

4. Discussion

Arthrofibrosis is a severe disabling postoperative complication after TKA which may lead to knee stiffness and constant pain. As the annual incidence of TKA rises into the millions [35−37], great attention should be paid to these symptoms since the increase of the arthrofibrosis prevalence worldwide. Unfortunately, there was no reliable biomarker for precise diagnosis and severity grading of arthrofibrosis. As such, the lack of indicators leads to a formidable

problem on the understanding of dynamic change during the whole process of pathogenesis. So, the arthrofibrosis biomarker is urgently needed in clinical practice.

Over the last decade, advances in genomics and biomarker assay techniques resulted in the identification of novel biomarkers. Current biomarkers of AF can be majorly categorized into two groups: serum-based biomarkers and tissue-based biomarkers. Serum-based biomarkers such as Eotaxin3, IL-5, IL12_23p40, IP10, VEGF, IL-7, IL-12p70, IL-16, and IL-17a are easy to obtain in the early stage of AF [38,39]. They were relatively easy to obtain and monitor the dynamic change during AF pathological process. However, they were largely reflections of the inflammation in the circulatory system and not
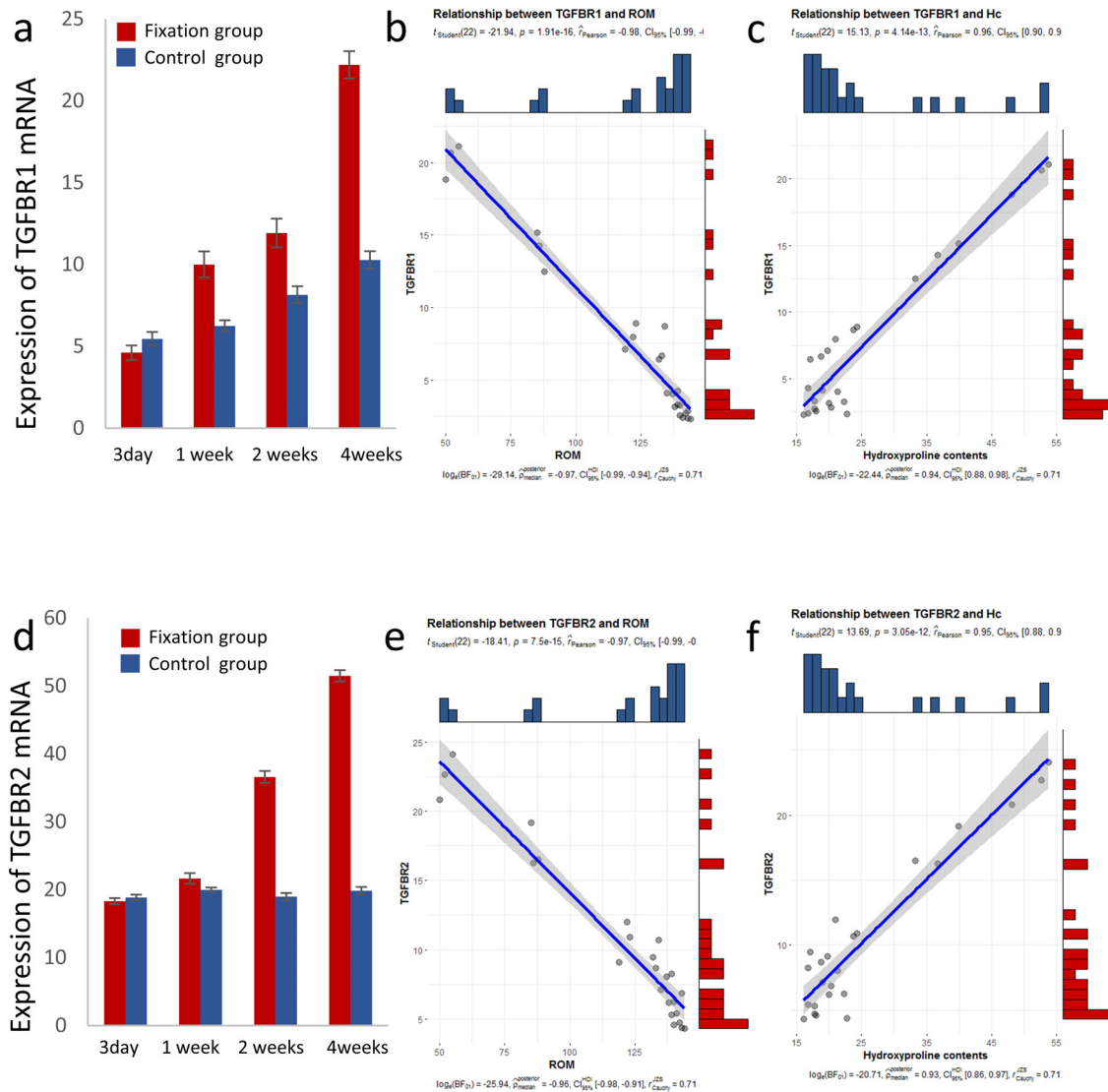
Fig. 4. Analysis of TGFBR1 and TGFBR2 expression in animal model.

　(a,d) Expression of the TGFBR1 and TGFBR2 mRNA in different fixation groups (*n*=12). Error bars indicate the standard deviations.

　(b,c,e,f) Correlation analysis between the TGFBR1 expression and ROM; TGFBR1 expression and Hydroxyproline contents; TGFBR2 expression and ROM; TGFBR2 expression and Hydroxyproline contents.

Table 3

Characteristic of baseline information of enrolled patients.

Parameter	Arthrofibrosis group (mean±SD)	Non-arthrofibrosis group (mean±SD)	*P*-value
Number of patients	46	92	-
Age(year)	67.04±12.17	68.59±11.62	1
Gender(male/female)	21/25	42/50	1
BMI(kg/m²)	24.41±4.43	23.62±3.74	0.06
affection side(left/right)	19/27	45/47	0.77
Baseline VAS	7.28	6.17	4.2E-05
Baseline ROM	78.58±7.42	128.26±13.79	2.2E-16

Table 4

ROC curve of the diagnosis test.

Indicators	Parameters	Values
TGFBR1	AUC (95%CI)	0.838[0.781−0.902]
	Sensitivity	0.638
	Specificity	0.913
	Cutoff point	1.500
TGFBR2	AUC (95%CI)	0.777[0.724−0.870]
	Sensitivity	0.511
	Specificity	0.903
	Cutoff point	2.500
α-SMA	AUC (95%CI)	0.711[0.627−0.795]
	Sensitivity	0.447
	Specificity	0.913
	Cutoff point	2.500

specific enough for the reflection of the focal adhesion formation. Tissue-based biomarkers included α-SMA (ASMA), Beta-catenin, CD68, MMPs, TIMPs and ADAMTS [8−12,27,40]. Although the synovial tissues are hard to get in clinical practice, they are more correlated to the clinical severity grading of AF and may contribute to the understanding of AF pathogenesis and drug discovery.

　In this study, we identified Transforming growth factor-β (TGF-β) receptor type 1 (TGFBR1) as the novel tissue-based biomarker via bioinformatic analysis of RNA-sequencing results and validated in

the animal model and clinical scenario. As the key component in the TGF-β/Smad signaling pathway, TGFBR1 was over-expressed in the AF groups comparing with the control in animal models. Clinical diagnosis test also manifested that the TGFBR1 is a promising indicator for arthrofibrosis with the significantly higher AUC (0.838) over α-SMA (0.711). As a well-known biomarker, α-SMA has been
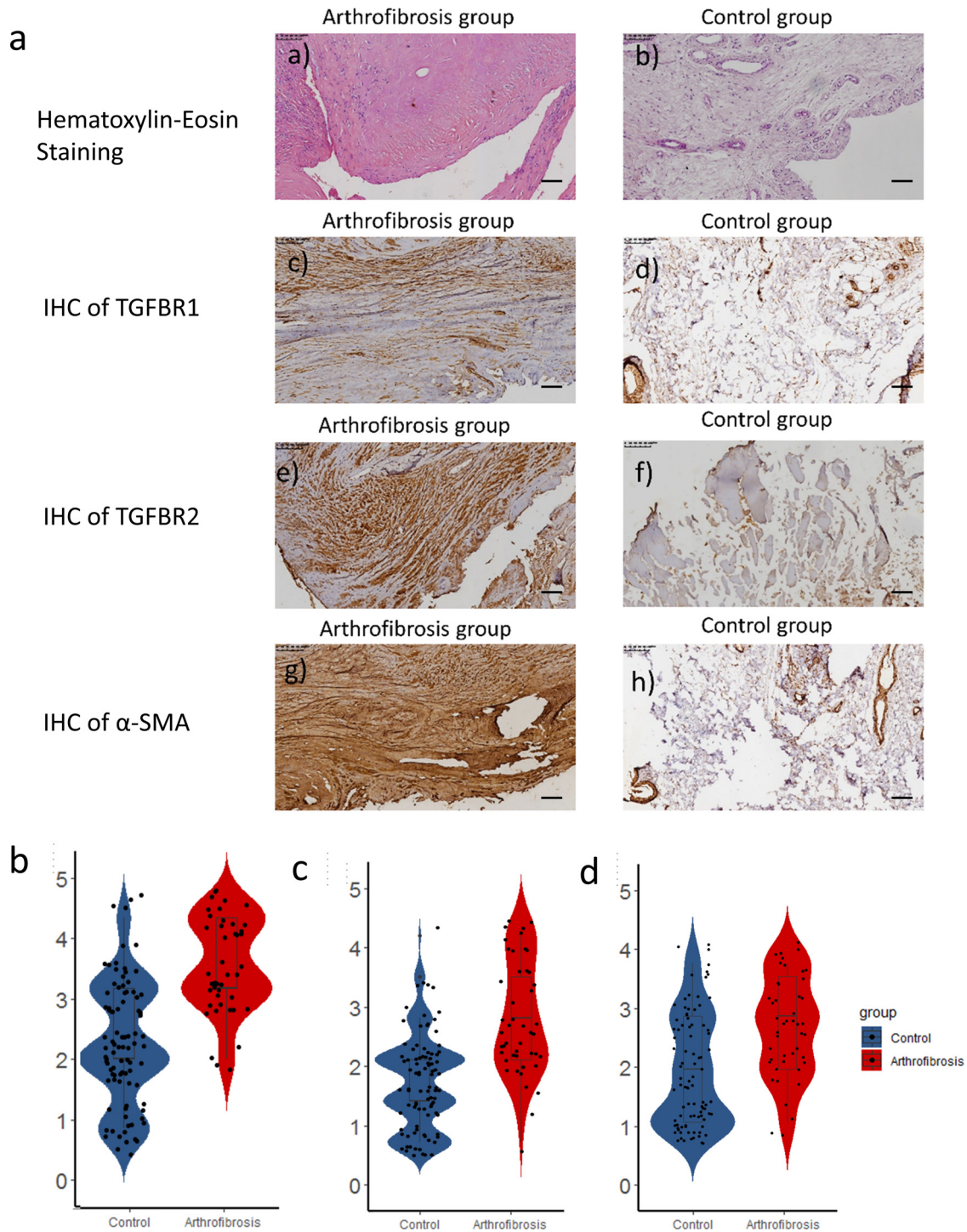
Fig. 5. Validation of biomarkers in the clinical patients with AF

(a) Representative histological slices of patients' synovial membrane tissue in the arthrofibrosis group and the control group stained by Hematoxylin-Eosin and immunohistochemistry. Bar = 200 μm.

(b–d) Violin plot of the TGFBR1, TGFBR2, and α-SMA score comparing with the Arthrofibrosis group (n=46) and the control group (n=92). The scatter points represent every single data of these two groups.

illustrated to be a reliable indicator of myofibroblasts differentiation in AF [8−10]. However, in the late stage of AF, the myofibroblasts may induce apoptosis or revert to origin cell types [7,41]. This will influence the accuracy of the AF severity grading by α-SMA stains [9]. Comparing with α-SMA, TGFBR1 also performed a higher correlation coefficient with ROM and VAS measurement both in the animal models and in clinical samples. According to previous studies [42], this

pain after TKA surgery may be caused by TGF-β1 induced nerve growth factor (NGF) via the TGFBR1-Smad2/3 signal pathway [42]. The mechanism of the correlation between TGFBR1 and knee pain remained indeterminate for further investigation.

In addition, our study suggested that TGFBR1 might act as a key part of pathogenesis and promising therapeutic target for arthrofibrosis (Fig. 7). When induced by TGF-β ligands, the up-regulated
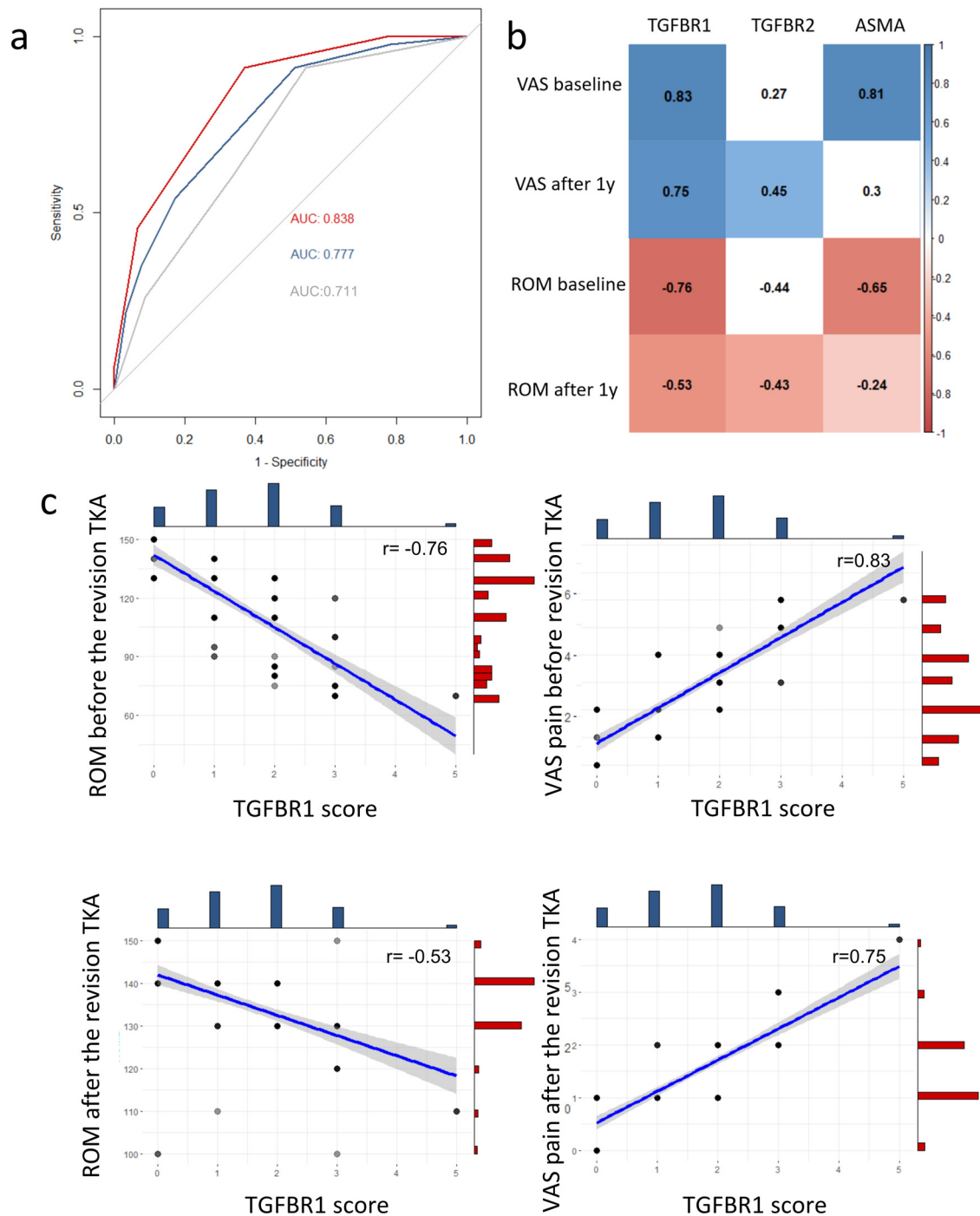
Fig. 6. Diagnosis test of TGFBR1 and TGFBR2

(a) ROC curve of TGFBR1 score model (colored red), ROC curve of TGFBR2 score model (colored blue), and ROC curve of α-SMA score model (colored grey)

(b) Correlation coefficient matrix of the TGFBR1 score, TGFBR2 score, and α-SMA score with the clinical outcome including ROM before revision surgery, VAS before revision surgery, ROM 12 months after the revision surgery, and VAS 12 months after the revision surgery. The color filled in the matrix represents the *p*-value of the correlation test (Pearson test).

(c) Correlation analysis between (a) TGFBR1 score and ROM before revision surgery; (b) TGFBR1 score and VAS before revision surgery; (c)TGFBR1 and ROM 12 months after the revision surgery; (c)TGFBR1 and VAS 12 months after the revision surgery (For interpretation of the references to color in this figure legend, the reader is referred to the web version of this article.).

TGFBR1 was bind to TGF-β receptor type 2 (TGFBR2) and activated [43]. The activated TGFBR1 consequently phosphorylated specific receptor-regulated SMADs (Smad2/3) and activated the canonical SMAD pathway to regulate gene transcription in the nucleus [44]. Moreover, the TGFBR1 can also activate other non-canonical signaling pathways, such as PI3K (phosphatidylinositol-3-kinase), MAPK

(mitogen-activated protein kinase), and AKT (a serine/threonine kinase) pathways [44−47]. Through the interplay and cross-talk of TGFBR1 signal mediators, the myofibroblasts were activated and ECM synthesis was increased which leading to the fibrogenesis in AF.

Interestingly, recent studies reported that the over-expressed TGFBR1 was sufficient to activate the downstream targets regardless
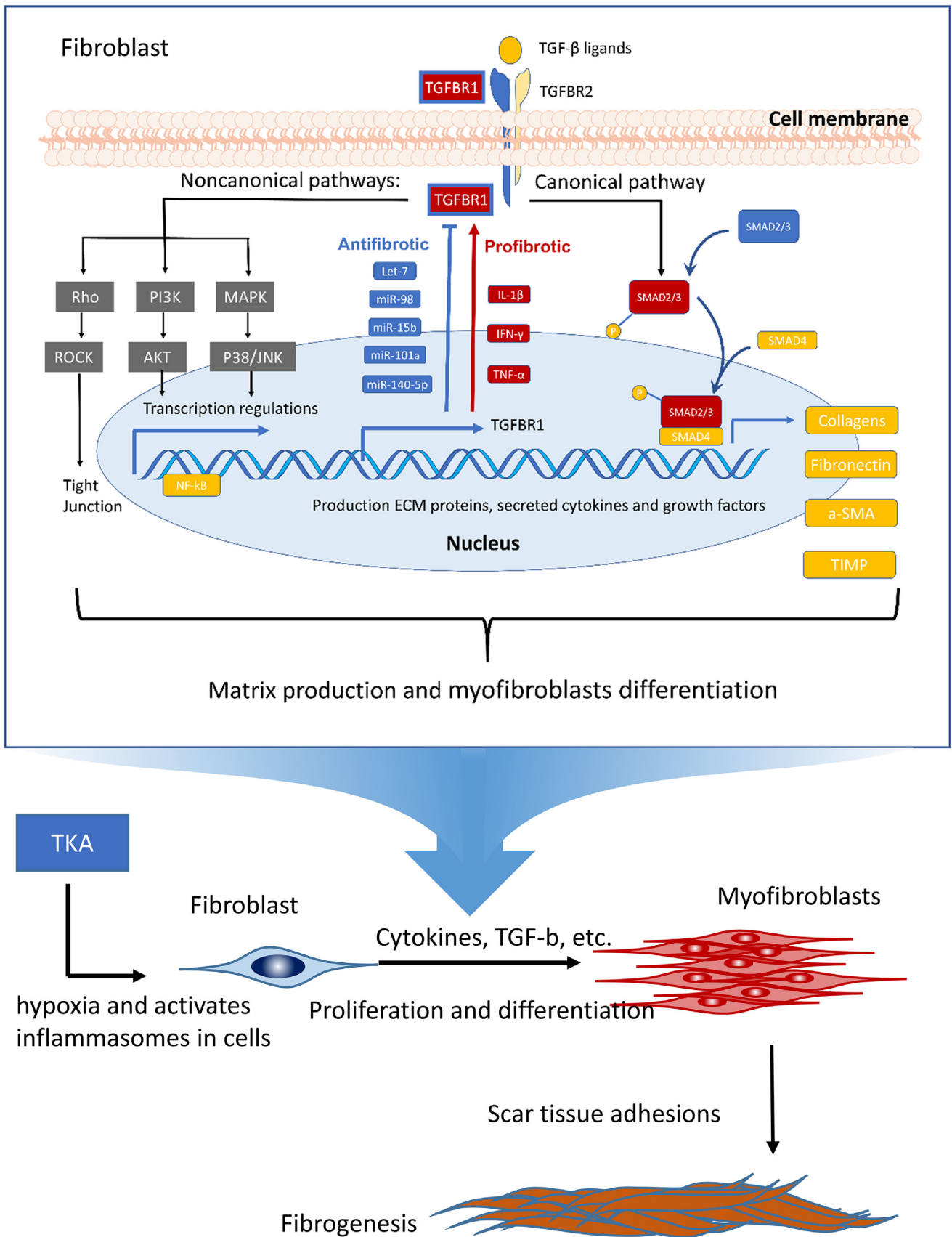
Fig. 7. Schematic of the proposed mechanism of TGFBR1 in arthrofibrosis after TKA.

The TGF-β signaling pathway starts with TGFBR1 binding with TGFBR2 when induced by the TGF-β ligands. Then, the kinase activity of TGFBR1 is activated, which phosphory-lated SMAD2/3 (Canonical pathway) and non-canonical downstream components (Non-canonical pathways). The activated SMAD2/3 can form a complex with SMAD4 and translo-cate to the nucleus. These signaling factors lead to the expression of profibrotic genes including collagens, fibronectin, α-smooth muscle actin (α-SMA), and tissue inhibitor of

of the amount of the ligands [48]. It is also known that the mixture of cytokine (such as IL-1β, TNF-α, and IFN-γ) can significantly up-regulate the expression of TGFBR1 [49]. Thus, we hypothesized that the up-regulated TGFBR1 may be an independent factor to induce arthrofibrosis without the TGF-β ligand activation. Previous studies manifested that the knockdown of TGFBR1 blocked proliferation and differentiation of fibroblasts in many other organs via inhibition of the TGF-β signal pathway, including cardiac fibrosis and renal fibrosis [50−52]. Other studies also reported that skin sclerosis was promoted by TGFBR1 which enhancing the TGF-β/Smad3 signaling pathways [53].

These results all supported that TGFBR1 could be a promising target for AF treatment. In fact, micro RNA-15b, micro RNA 140−5p, micro RNA-98, micro RNA-101a, and Let-7b targeting to down-regulate the TGFBR1 had already shown therapeutic effect of the fibrosis of kidney, liver, and cardiac [50,51,54−56]. Whereas the application of TGFBR1 inhibitors was limited in other fibrosis diseases due to the side effect addressed by previous studies such as liver and cardiac toxicity when systematical used of TGFBR1 [57−59]. But Intra-articular usage of medication can regulation the TGFBR1 expression specifically in the knee cavity which will reduce the adverse effect and benefit for patients with AF. Recently, Lee and his colleagues have demonstrated that sustained delivery of TGFBR1 inhibitor (SB-431,542) will down-regulated the α-smooth muscle actin expression and connective tissue growth factor production [60].

The present study had the following shortcomings: First, the number of patients involving in these two groups was restricted to the minimum number according to the experiment design, which was relatively small. Despite the limited number, this study can still be generalized to the wider population base on the different levels of validations in RNA-seq samples, animal model samples, and clinical samples. The various populations of this study, including American patients for bioinformatic analysis and Asian patients for validation, also guarantee the extrapolability of other populations. Second, we only evaluated the mRNA expression of TGFBR1 and TGFBR2 in the animal model. Further work is still required to measure the protein level of the TGFBR1 and TGFBR2, to clarify the regulation of these functions, and to explore the underlying mechanisms of arthrofibrosis development. Moreover, this study only involved the synovial membrane tissues. The aim of our study was not only to identify a novel biomarker but also a therapeutic target for drug discovery. With this, we mainly focus on the tissue-based biomarker in this study. We will manage to collect other samples such as peripheral blood and synovial fluid to confirm these results from another perspective which may extend its application in the future.

In this study, we identified the TGFBR1 as a potential biomarker for diagnosis, severity rating, and prognosis prediction of arthrofibrosis. High-level of TGFBR1 in the patients suggest the severity of the disease and less ROM after surgery. It also implied more pain reported by patients both before and after the revision surgery. This may lead to a worse prognosis and dissatisfaction of patients which requires careful attention of the surgeons.

Author contributions

M.C. and Y.X.Z. designed the experiments; X.C. and Z.L.W. performed the experiments; X.C., H.Y., W.D., and Z.L.W. analyzed the data; X.C., H.Y., W.D., and Z.L.W verified the data; X.C. wrote the manuscript; M.C. and Y.X.Z. revised the manuscript. All authors read and approved the final manuscript.

Declaration of Competing Interest

These authors declare no competing interests.

Data sharing statement

All data is available in the main text or supplementary materials. The RNA-Seq dataset was available at NCBI GEO (GSE135854). All data, models, code generated or used during the study are available from the corresponding author upon reasonable request.

Supplementary materials

Supplementary material associated with this article can be found in the online version at doi:10.1016/j.ebiom.2021.103486.

References

[1] Cheuy VA, Foran JRH, Paxton RJ, Bade MJ, Zeni JA, Stevens-Lapsley JE. Arthrofibrosis associated with total knee arthroplasty. J Arthroplast 2017;32(8):2604. 11.
[2] Rutherford RW, Jennings JM, Levy DL, Parisi TJ, Martin JR, Dennis DA. Revision total knee arthroplasty for arthrofibrosis. J Arthroplast 2018;33(7S):S177. S81.
[3] Tibbo ME, Limberg AK, Salib CG, et al. Acquired idiopathic stiffness after total knee arthroplasty: a systematic review and meta-analysis. J Bone Jt Surg Am 2019;101 (14):1320. 30.
[4] Cohen JS, Gu A, Lopez NS, Park MS, Fehring KA, Sculco PK. Efficacy of revision surgery for the treatment of stiffness after total knee arthroplasty: a systematic review. J Arthroplast 2018;33(9):3049. 55.
[5] Pitta M, Esposito CI, Li Z, Lee YY, Wright TM, Padgett DE. Failure after modern total knee arthroplasty: a prospective study of 18,065 knees. J Arthroplast 2018;33(2):407. 14.
[6] Cregar WM, Khazi ZM, Lu Y, Forsythe B, Gerlinger TL. Lysis of adhesion for arthrofibrosis after total knee arthroplasty is associated with increased risk of subsequent revision total knee arthroplasty. J Arthroplast 2021;36(1):339. 44 e1.
[7] Usher KM, Zhu S, Mavropalias G, Carrino JA, Zhao J, Xu J. Pathological mechanisms and therapeutic outlooks for arthrofibrosis. Bone Res 2019;7:9.
[8] Unterhauser FN, Bosch U, Zeichen J, Weiler A. Alpha-smooth muscle actin containing contractile fibroblastic cells in human knee arthrofibrosis tissue. Winner of the AGA-DonJoy Award 2003. Arch Orthop Trauma Surg 2004;124(9):585. 91.
[9] Ruppert M, Theiss C, Knoss P, et al. Histopathological, immunohistochemical criteria and confocal laser-scanning data of arthrofibrosis. Pathol Res Pract 2013;209(11):681. 8.
[10] Mayr HO, Fassbender FF, Prall WC, Haasters F, Bernstein A, Stoehr A. Immunohistochemical examination in arthrofibrosis of the knee joint. Arch Orthop Trauma Surg 2019;139(3):383. 91.
[11] Bresnihan B, Pontifex E, Thurlings RM, et al. Synovial tissue sublining CD68 expression is a biomarker of therapeutic response in rheumatoid arthritis clinical trials: consistency across centers. J Rheumatol 2009;36(8):1800. 2.
[12] Mann CJ, Bradley AM, Jones ER, McNamara IR, Smith TO, Riley GP. Stiffness post-total knee replacement: a proof of principle study investigating the effect of gene expression analysis of markers of fibrosis. Knee 2019;26(4):914. 22.
[13] Bayram B, Limberg AK, Salib CG, et al. Molecular pathology of human knee arthrofibrosis defined by RNA sequencing. Genomics 2020;112(4):2703. 2.

matrix metalloproteinases (TIMP). Other TGFβ-induced non-Smad signaling pathways include PI3K-AKT, the small GTPases Rho and MAPK pathways can also regulate the transcription and induce matrix deposition.

In the setting of tissue injury, as in TKA, fibroblasts are stimulated by hypoxia and activates inflammasomes in cells. The mixture of cytokines (IL-1β, TNF-α, and IFN-γ) upregulate the TGFBR1 while the TGF-b activates this signal pathway. These events stimulate fibroblasts to proliferation and differentiate into myofibroblasts which promote contraction and the upregulation of ECM protein production. The excessive ECM and focal adhesions become more complex and form fibrotic scar over time.

Abbreviations in the figure: P in the yellow circle, serine/threonine kinase phosphorylation. TGFBR1, Transforming growth factor-beta receptor 1. TGFBR2, Transforming growth factor-beta receptor 2. ROCK, Rho-associated coiled-coil containing protein kinase. PI3K, phosphoinositide 3-kinase. AKT, v-akt murine thymoma viral oncogene homologue 1. MAPK, mitogen-activated protein kinase. JNK, c-Jun N-terminal kinase. IL-1β, interleukin-1β. TNF-α, tumor necrosis factor α. IFN-γ, Interferon γ. miR, micro RNA.

[14] Hildebrand KA, Sutherland C, Zhang M. Rabbit knee model of post-traumatic joint contractures: the long-term natural history of motion loss and myofibroblasts. J Orthop Res 2004;22(2):313. 20.

[15] Wang J, Yan L, Sun Y, et al. A comparative study of the preventive effects of mito-mycin C and chitosan on intraarticular adhesion after knee surgery in rabbits. Cell Biochem Biophys 2012;62(1):101. 5.

[16] Sun Y, Liang Y, Hu J, et al. Reduction of intraarticular adhesion by topical application of colchicine following knee surgery in rabbits. Sci Rep 2014;4:6405.

[17] Arsoy D, Salib CG, Trousdale WH, et al. Joint contracture is reduced by intra-articular implantation of rosiglitazone-loaded hydrogels in a rabbit model of arthrofibrosis. J Orthop Res 2018;36(11):2949. 55.

[18] Zhou Y, Yang K. Prevention of arthrofibrosis during knee repair by extracorporeal shock wave therapy: preliminary study in rabbits. Injury 2019;50(3):633. 8.

[19] Zhou Y, Zhang QB, Zhong HZ, et al. Rabbit model of extending knee joint contracture: progression of joint motion restriction and subsequent joint capsule changes after immobilization. J Knee Surg 2020;33(1):15–21.

[20] Hazlewood D, Feng Y, Lu Q, Yang X, Wang J. Novel rabbit model of moderate knee contracture induced by direct capsular damage. J Orthop Res 2018;36(10):2687. 95.

[21] National Research Council. Guide for the care and use of laboratory animals. Washington, DC: The National Academies Press; 1996.

[22] Kolde R. Pheatmap: Pretty Heatmaps, R Package Version 1.0.12. 2019. (http://CRAN.Rproject.org/package=pheatmap 2019)

[23] Szklarczyk D, Gable AL, Nastou KC, et al. The STRING database in 2021: customizable protein-protein networks, and functional characterization of user-uploaded gene/measurement sets. Nucleic Acids Res 2021;49(D1):D605. D12.

[24] Szklarczyk D, Franceschini A, Kuhn M, et al. The STRING database in 2011: functional interaction networks of proteins, globally integrated and scored. Nucleic Acids Res 2011;39:D561. Database issue8.

[25] Nesterenko S, Morrey ME, Abdel MP, An KN, Sanchez-Sotelo J. New rabbit knee model of posttraumatic joint contracture: indirect capsular damage induces a severe contracture. J Orthop Res 2009;27(8):1028. 32.

[26] Wong K, Sun F, Trudel G, Sebastiani P, Laneuville O. Temporal gene expression profiling of the rat knee joint capsule during immobilization-induced joint contractures. BMC Musculoskelet Disord 2015;16:125.

[27] Faust I, Traut P, Nolting F, et al. Human xylosyltransferases–mediators of arthrofibrosis? New pathomechanistic insights into arthrofibrotic remodeling after knee replacement therapy. Sci Rep 2015;5:12537.

[28] von Elm E, Altman DG, Egger M, Pocock SJ, Gøtzsche PC, Vandenbroucke JP. The strengthening the reporting of observational studies in epidemiology (STROBE) statement: guidelines for reporting observational studies. Annals Intern Med 2007;147(8):573. 7.

[29] Gandhi R, de Beer J, Leone J, Petruccelli D, Winemaker M, Adili A. Predictive risk factors for stiff knees in total knee arthroplasty. J Arthroplast 2006;21(1):46–52.

[30] Boldt JG, Stiehl JB, Hodler J, Zanetti M, Munzinger U. Femoral component rotation and arthrofibrosis following mobile-bearing total knee arthroplasty. Int Orthop 2006;30(5):420. 5.

[31] Hawker GA, Mian S, Kendzerska T, French M. Measures of adult pain: visual analog scale for pain (VAS Pain), numeric rating scale for pain (NRS Pain), mcgill pain questionnaire (MPQ), short-form mcgill pain questionnaire (SF-MPQ), chronic pain grade scale (CPGS), short form-36 bodily pain scale (SF-36 BPS), and measure of intermittent and constant osteoarthritis pain (ICOAP). Arthritis Care Res (Hoboken) 2011;63:S240. **Suppl 11**52.

[32] Wickham H, Averick M, Bryan J, et al. Welcome to the Tidyverse. J Open Source Softw 2019;4(43):1686.

[33] Wei T, Simko V (2017) R package "corrplot": visualization of a correlation matrix. R package version 0.84 (https://Github.Com/Taiyun/Corrplot)

[34] Robin X, Turck N, Hainard A, et al. pROC: an open-source package for R and S+ to analyze and compare ROC curves. BMC Bioinform 2011;12(1):77.

[35] Banerjee S, Wright MD. CADTH rapid response reports. outpatient or short stay total hip or knee arthroplasty versus conventional total hip or knee arthroplasty: A review of clinical effectiveness, cost-effectiveness and guidelines. Ottawa (ON): Canadian Agency for Drugs and Technologies in Health; 2021 Copyright © 2020 Canadian Agency for Drugs and Technologies in Health.; 2020.

[36] Nemeth B, Nelissen R, Arya R, Cannegieter S. Preventing VTE following total hip and knee arthroplasty: Is prediction the future? J Thromb Haemost 2021;19(1):41. *JTH5*Copyright © 2021, StatPearls Publishing LLC.; 2021.

[37] Gemayel AC, Varacallo M. Total knee replacement techniques. StatPearls. Treasure Island (FL). StatPearls Publishing; 2021.

[38] Malahias MA, Birch GA, Zhong H, et al. Postoperative Serum cytokine levels are associated with early stiffness after total knee arthroplasty: a prospective cohort study. J Arthroplast 2020;35(6S):S336. S47.

[39] Wu J, Wang K, Xu J, et al. Associations between serum ghrelin and knee symptoms, joint structures and cartilage or bone biomarkers in patients with knee osteoarthritis. Osteoarthr Cartil 2017;25(9):1428. 35.

[40] Abdul N, Dixon D, Walker A, et al. Fibrosis is a common outcome following total knee arthroplasty. Sci Rep 2015;5:16469.

[41] Trautwein C, Friedman SL, Schuppan D, Pinzani M. Hepatic fibrosis: Concept to treatment. J Hepatol 2015;62(1):S15. Suppl24.

[42] Blaney Davidson EN, van Caam AP, Vitters EL, et al. TGF-beta is a potent inducer of nerve growth factor in articular cartilage via the ALK5-Smad2/3 pathway. Potential role in OA related pain? Osteoarthr Cartil 2015;23(3):478. 86.

[43] Miller DSJ, Bloxham RD, Jiang M, et al. The dynamics of TGF-beta signaling are dictated by receptor trafficking via the ESCRT machinery. Cell Rep 2018;25(7):1841. 55 e5.

[44] Mu Y, Gudey SK, Landstrom M. Non-Smad signaling pathways. Cell Tissue Res 2012;347(1):11–20.

[45] Barrios-Rodiles M, Brown KR, Ozdamar B, et al. High-throughput mapping of a dynamic signaling network in mammalian cells. Science 2005;307(5715):1621. 5.

[46] Vogelmann R, Nguyen-Tat MD, Giehl K, Adler G, Wedlich D, Menke A. TGFbeta-induced downregulation of E-cadherin-based cell-cell adhesion depends on PI3-kinase and PTEN. J Cell Sci 2005;118(Pt 20):4901. 12.

[47] Gomes LR, Terra LF, Wailemann RA, Labriola L, Sogayar MC. TGF-β1 modulates the homeostasis between MMPs and MMP inhibitors through p38 MAPK and ERK1/2 in highly invasive breast cancer cells. BMC Cancer 2012;12:26.

[48] Kim W, Kim E, Lee S, et al. TFAP2C-mediated upregulation of TGFBR1 promotes lung tumorigenesis and epithelial-mesenchymal transition. Exp Mol Med 2016;48(11):e273.

[49] Liu X. Inflammatory cytokines augments TGF-beta1-induced epithelial-mesenchymal transition in A549 cells by up-regulating TbetaR-I. Cell Motil Cytoskelet 2008;65(12):935. 44.

[50] Cheng R, Dang R, Zhou Y, Ding M, Hua H. MicroRNA-98 inhibits TGF-beta1-induced differentiation and collagen production of cardiac fibroblasts by targeting TGFBR1. Hum Cell 2017;30(3):192–200.

[51] Liao W, Liang P, Liu B, et al. MicroRNA-140-5p mediates renal fibrosis through TGF-beta1/Smad signaling pathway by directly targeting TGFBR1. Front Physiol 2020;11:1093.

[52] Zhang P, Cai Y, Soofi A, Dressler GR. Activation of Wnt11 by transforming growth factor-beta drives mesenchymal gene expression through non-canonical Wnt protein signaling in renal epithelial cells. J Biol Chem 2012;287(25):21290. 302.

[53] Yang T, Zhang X, Chen A, et al. Progranulin promotes bleomycin-induced skin sclerosis by enhancing transforming growth factor-beta/smad3 signaling through up-regulation of transforming growth factor-beta type I receptor. Am J Pathol 2019;189(8):1582. 93.

[54] Wang B, Jha JC, Hagiwara S, et al. Transforming growth factor-β1-mediated renal fibrosis is dependent on the regulation of transforming growth factor receptor 1 expression in let-7b. Kidney Int 2014;85(2):352. 61.

[55] Zhao X, Wang K, Liao Y, et al. MicroRNA-101a inhibits cardiac fibrosis induced by hypoxia via targeting TGFbetaRI on cardiac fibroblasts. Cell Physiol Biochem 2015;35(1):213. 26.

[56] Tijsen AJ, van der Made I, van den Hoogenhof MM, et al. The microRNA-15 family inhibits the TGFβ-pathway in the heart. Cardiovasc Res 2014;104(1):61–71.

[57] Herbertz S, Sawyer JS, Stauber AJ, et al. Clinical development of galunisertib (LY2157299 monohydrate), a small molecule inhibitor of transforming growth factor-beta signaling pathway. Drug Des Dev Ther 2015;9:4479. 99.

[58] Mora AL, Rojas M, Pardo A, Selman M. Emerging therapies for idiopathic pulmonary fibrosis, a progressive age-related disease. Nat Rev Drug Discov 2017;16(11):810.

[59] Anderton MJ, Mellor HR, Bell A, et al. Induction of heart valve lesions by small-molecule ALK5 inhibitors. Toxicol Pathol 2011;39(6):916. 24.

[60] Lee AJ, Mahoney CM, Cai CC, et al. Sustained delivery of SB-431542, a type I transforming growth factor beta-1 receptor inhibitor, to prevent arthrofibrosis. Tissue Eng Part A 2021.